Inorganic Chemistry

Article

pubs.acs.org/IC

Dinuclear Ruthenium Complexes Containing the Hpbl Ligand: Synthesis, Characterization, Linkage Isomerism, and Epoxidation Catalysis

Laia Francàs,[†,‡] Rosa María González-Gil,[‡] Daniel Moyano,[‡] Jordi Benet-Buchholz,[†] Jordi García-Antón,[‡] Lluís Escriche,*[,‡] Antoni Llobet,*[,†,‡] and Xavier Sala*[,‡]

[†]Institute of Chemical Research of Catalonia (ICIQ), Av. Països Catalans 16, E-43007 Tarragona, Spain

[‡]Departament de Química, Universitat Autònoma de Barcelona, Cerdanyola del Vallès, 08193 Barcelona, Spain

Supporting Information

ABSTRACT: Three dinucleating Ru−Cl complexes containing the hexadentate dinucleating ligand [1,1′-(4-methyl-1*H*-pyrazole-3,5-diyl)bis(1-(pyridin-2-yl)ethanol)] (Hpbl) and the meridional 2,2′:6′,2″-terpyridine ligand (trpy) have been prepared and isolated. These complexes include $\{[RuCl(trpy)]_2(\mu\text{-pbl-}\kappa\text{-N}^3O)\}^+$ ($\mathbf{1a}^+$), $\{[RuCl(trpy)]_2(\mu\text{-Hpbl-}\kappa\text{-N}^3O)\}^{2+}$ ($\mathbf{1b}^{2+}$), and $\{[RuCl(trpy)]_2(\mu\text{-Hpbl-}\kappa\text{-N}^2O^2)\}^{2+}$ ($\mathbf{1c}^{2+}$) and were characterized by analytic and spectroscopic techniques. In addition, complexes $\mathbf{1b}^{2+}$ and $\mathbf{1c}^{2+}$ were characterized in the solid state by monocrystal X-ray diffraction analysis. The coordination versatility of the Hpbl ligand allows the presence of multiple isomers that can be obtained depending on the Ru oxidation state and were thoroughly characterized by electrochemical techniques, namely, cyclic voltammetry and coulometry. Finally, $\mathbf{1a}^+$ and its recently reported mononuclear analogue, *in*-$[RuCl(Hpbl)(trpy)]^+$, have been tested as catalysts for epoxidation of *cis*-*β*-methylstyrene.

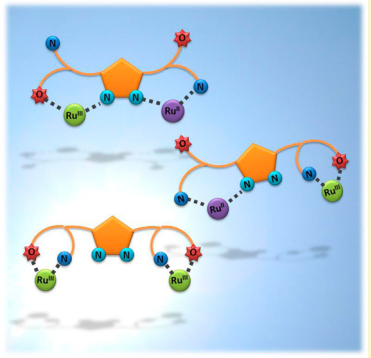

INTRODUCTION

Redox catalysts play a prominent role in the selective preparation of versatile intermediates for organic synthesis, as is the case, for instance, in the regio- and/or stereoselective transformation of double bonds into epoxides.[1] The epoxides are extremely useful molecules for both the chemical industry (particularly in polymer manufacture)[2] and the synthesis of fine chemicals, such as pharmaceuticals, food additives, or flavor and fragrances.[3] On the other hand, water oxidation redox catalysis is one of the major topics that need to be dominated in order to come up with new energy conversion schemes that allow the transition from fossil to solar fuels.[4]

Mono- and dinuclear Ru complexes based on $Ru^{II}-OH_2$/$Ru^{IV}=O$ motifs, achievable via proton-coupled electron transfer (PCET) processes,[5] have been thoroughly studied as redox catalysts. A number of oxidative transformations including the ones mentioned above have been described. We recently contributed to this chemistry[6] focusing our attention at the influence of metal cooperation over catalysis.[7] For this purpose, several dinucleating ligands (Chart 1) have been used as bridges between two Ru metal centers, and the catalytic properties of the resulting complexes have been studied for reactions of water oxidation and alkene epoxidation.[8]

A key issue for this type of chemistry is the need to cycle among different oxidation states, such as, for instance, Ru(II) and Ru(V), while keeping a stable coordination environment.[9] In order to come up with ligands that can stabilize low and high oxidation states we recently reported a new dinucleating bridging ligand with N/O ambidentate motifs (Hpbl, Chart 1) and its mononuclear Ru complexes. We have shown that when oxidation state III is reached it undergoes N → O linkage

Chart 1. Drawing of the Ligands Used in This Work (right) and Dinucleating Bridging Ligands Previously Employed To Induce Metal Cooperation (left)

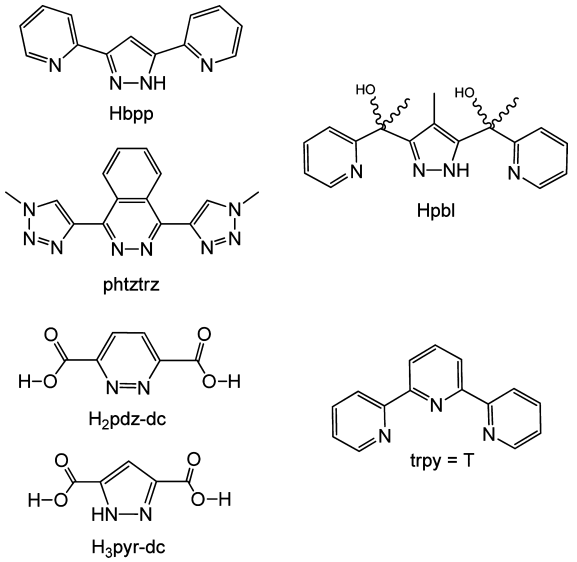

Received: June 20, 2014
Published: September 25, 2014

 © 2014 American Chemical Society dx.doi.org/10.1021/ic501483s | *Inorg. Chem.* 2014, 53, 10394−10402

isomerization, drastically reducing redox potentials of high oxidation states.[10]

Herein, we report the coordination chemistry and linkage isomerization processes of dinuclear Ru−Hpbl complexes of general formula $\{[RuCl(trpy)]_2(\mu\text{-pbl})\}^{n+}$, together with their catalytic properties with regard to epoxidation of *cis*-β-methylstyrene. In addition, the epoxidation capacity of their mononuclear Ru−Hpbl counterparts is also reported and compared to related complexes previously reported in the literature (Chart 1).

EXPERIMENTAL SECTION

Materials. All reagents used in the present work were obtained from Sigma-Aldrich Chemical Co. and used without further purification. Reagent-grade organic solvents were obtained from SDS. $RuCl_3{\cdot}3H_2O$ was supplied by Alfa Aesar and used as received.

Instrumentation and Measurements. UV−vis spectroscopy was performed by a HP8453 spectrometer using 1 cm quartz cells. NMR spectroscopy was performed on a Bruker DPX 250 MHz, DPX 360 MHz, or a DPX 400 MHz spectrometer. Gas chromatography (GC) was performed in an Agilent 6890N with a mass-selective detector with ionization by electronic impact or in an Agilent 6890 GC with a flame ionization detector (FID) detector using a HP5 column. Electrospray ionization mass spectrometry (ESI-MS) experiments were carried out on a microTOF-Q system from Bruker Daltonics at the Servei d'Anàlisi Química of the Universitat Autònoma de Barcelona (SAQ-UAB).

Cyclic voltammetry (CV) experiments were performed on PAR283 potentiostat, IJ-Cambria HI-660 potentiostat, or BioLogic potentiostat/galvanostat and EC-Lab software using a three-electrode cell. A glassy carbon electrode (3 mm diameter) was used as working electrode, platinum wire as auxiliary electrode, and SSCE as a reference electrode. Working electrodes were polished with 0.05 μm alumina paste washed with distilled water and acetone before each measurement. $E_{1/2}$ values reported in this work were estimated from CV experiments as the average of the oxidative and reductive peak potentials $(E_{p,a} + E_{p,c})/2$. All electrochemical measurements are performed in MeOH with 0.1 M $n\text{-}Bu_4N^+PF_6^-$ (TBAH) as supporting electrolyte.

Epoxidation catalytic experiments were performed as follows. A solution of 1.25×10^{-3} mmol of dinuclear catalyst (or 2.50×10^{-3} mmol of mononuclear), 1.60 g (5.0 mmol) of (diacetoxyiodo)benzene $(PhI(OAc)_2)$, 1 mmol of biphenyl, and 90 μL (5.0 mmol) of water were dissolved in 1 mL of 1,2-dichloroethane (DCE) and allowed to stir for 2 h. Then 2.5 mmol of substrate were added, reaching a final volume of approximately 1.4 mL. Aliquots were taken every 5, 10, 15, 20, 25, 30 min or until the reaction was completed. Each aliquot was filtered through a Pasteur pipet filled with Celite and rinsed with diethyl ether. The filtrate was analyzed by GC and GC-MS.

Preparation. The starting complex $[RuCl_3(trpy)]$[11] and the Hpbl ligand [1,1′-(4-methyl-1*H*-pyrazole-3,5-diyl)bis(1-(pyridin-2-yl)-ethanol)][10] were prepared as described in the literature. All synthetic manipulations were routinely performed under nitrogen atmosphere using Schlenck tubes and vacuum line techniques.

{[RuCl(trpy)]$_2$(μ-pbl-κ-N^{3}O)}(PF$_6$), ***1a(PF$_6$)***. A sample of 200 mg (0.454 mmol) of $[RuCl_3(trpy)]$ and 61 mg (1.439 mmol) of LiCl was dissolved in 20 mL of dry MeOH containing 250 μL (1.816 mmol) of NEt_3. The mixture was stirred at room temperature (RT) for 20 min, and then 74 mg (0.228 mmol) of Hpbl in 2.4 mL of a 0.29 M MeONa solution (0.685 mmol) were added. The mixture was refluxed under stirring for 24 h. Alternatively, the reaction can also be performed in a microwave reactor by carrying out five 10 min heating cycles (75 °C/300 W) with 5 min of equilibration time between them. The mixture was filtered, and 2 mL of a saturated NH_4PF_6 aqueous solution and 5 mL of water were added to the filtrate. Then, the volume was reduced on a rotary evaporator until a precipitate appeared, which was filtered off and dried. The obtained solid was partially dissolved in hot CH_2Cl_2, and the solution was cooled down. The remaining solid was filtered off, washed with water and diethyl ether, and vacuum dried. Yield: 75 mg (27%) for the reflux reaction; 100 mg (36%) for the microwave reaction. ESI-HRMS (MeOH): m/z = 1205.0500 ($[M]^+$). CV (MeOH/TBAH) $E_{1/2}$ = 0.07 V; $E_{1/2}$ = 0.77 V. OCP: 0.1 V. Anal. Calcd for $C_{48}H_{40}Cl_2F_6N_{10}O_2PRu_2$: C, 47.77; H, 3.34; N, 11.61. Found: C, 47.52; H, 3.45; N, 11.37. UV−vis (MeOH) [λ_{max}, nm (ε, M^{-1} cm^{-1})]: 276 (26 822), 283 (25 083), 320 (28 868), 379 (8637), 516 (5148), 585 (5956).

{[RuCl(trpy)]$_2$(μ-pbl-κ-N^{3}O)}$^+$, ***1aH$^+$***. This complex was obtained in situ by adding ascorbic acid to a MeOD solution of $\mathbf{1a}^+$. ^{1}H NMR (500 MHz, MeOD + ascorbic acid): δ = 10.01 (d, 1H$_1$, $^3J_{1-2}$ = 5.62 Hz), 8.60−8.40 (m, 8H$_{trpy}$), 8.26 (d, 1H$_{trpy}$), 8.17 (t, 1H$_{trpy}$), 8.08 (t, 2H$_{trpy}$), 8.00−7.88 (m, 7H$_{trpy,2,8}$), 7.80 (t, 1H), 7.74 (d, 1H$_4$, $^3J_{4-3}$ = 5.50 Hz), 7.66 (d, 1H$_{trpy}$), 7.56 (t, 1H$_{trpy}$), 7.50 (ddd, 1H$_9$, $^3J_{9-8}$ = 8.50 Hz, $^4J_{9-10}$ = 7.30 Hz, $^5J_{9-11}$ = 1.44 Hz), 7.40 (t, 1H$_{trpy}$), 7.27 (ddd, 1H$_3$, $^3J_{3-2}$ = 7.70 Hz, $^4J_{3-4}$ = 5.50 Hz, $^5J_{3-1}$ = 1.10 Hz), 7.25 (d, 1H$_{11}$, $^3J_{11-10}$ = 5.80 Hz), 6.61 (ddd, 1H$_{10}$, $^3J_{10-9}$ = 7.30 Hz, $^4J_{10-11}$ = 5.80 Hz, $^5J_{10-8}$ = 1.50 Hz), 2.14 (s, 3H$_6$), 1.67 (s, 3H$_5$), 1.44 (s, 3H$_7$). UV−vis (MeOH) [λ_{max}, nm (ε, M^{-1} cm^{-1})]: 280 (26 692), 282 (27 401), 320 (33 910), 379 (9798), 489 (6321), 527 (6166).

{[RuCl(trpy)]$_2$(μ-Hpbl-κ-N^{3}O)}(PF$_6$)$_2$, ***1b(PF$_6$)$_2$***. A sample of 50 mg (0.04 mmol) of $\mathbf{1a(PF_6)}$ was dissolved in 50 mL of MeOH. The mixture was left stirring at room temperature for 1 week. Then, saturated aqueous NH_4PF_6 (0.2 mL) and water (0.5 mL) were added to the solution, and the volume was reduced on a rotary evaporator. The solution was cooled at −33 °C overnight. A brown precipitate appeared, which was filtered off and washed with cold methanol and dried with diethyl ether. Yield: 35 mg (65%). ESI-MS (MeOH): m/z = 531.5 ($[M - 2PF_6]^{2+}$). CV (MeOH/TBAH): $E_{1/2}$ = 0.3 V; $E_{1/2}$ = 0.77 V. OCP: 0.465 V. Anal. Calcd for $C_{48}H_{41}Cl_2F_{12}N_{10}O_2P_2Ru_2$: C, 42.61; H, 3.05; N, 10.35. Found: C, 42.47; H, 3.04; N, 10.23. UV−vis (MeOH) [λ_{max}, nm (ε, M^{-1} cm^{-1})]: 275 (34 171), 281 (32 372), 318 (30 894), 377 (7216), 475 (5088), 513 (4062).

{[RuCl(trpy)]$_2$(μ-Hpbl-κ-N^{2}O^2)}(PF$_6$)$_2$·MeOH, ***1c(PF$_6$)$_2$·MeOH***. A sample of 50 mg (0.040 mmol) of $\mathbf{1a(PF_6)}$ and 24.02 mg (0.044 mmol) of $Ce(NO_3)_6(NH_4)_2$ was dissolved in 50 mL of methanol. The mixture was stirred at room temperature for 4 days under nitrogen atmosphere. Then, the mixture was filtered, and the solvent was evaporated and replaced by CH_2Cl_2. The insoluble portion was filtered off, and the filtered solution was washed with 20 mL of water plus 20 mL of a saturated NaCl solution. The organic fraction was then dried with anhydrous Na_2SO_4, filtered, and evaporated to dryness. The residue was redissolved in methanol, and 0.2 mL of a saturated aqueous solution of NH_4PF_6 was added together with 0.5 mL of water. The volume was then reduced on a rotary evaporator until a precipitate appeared, and the remaining solution was cooled at −33 °C overnight. The brown solid formed was filtered off, washed with cold methanol, and dried with diethyl ether and under vacuum. Yield: 11 mg (20%). CV (MeOH/TBAH) $E_{1/2}$ = 0.30 V. OCP: 0.468 V. Anal. Calcd for $C_{49}H_{44}Cl_2F_{12}N_{10}O_3P_2Ru_2$: C, 42.53; H, 3.20; N, 10.12. Found: C, 42.47; H, 3.04; N, 10.23. UV−vis (MeOH) [λ_{max}, nm (ε, M^{-1} cm^{-1})]: 317 (24 000), 328 (21 284), 411 (5028), 444 (4616). ESI-MS (MeOH): m/z = 531.0 ($[M - 2PF_6]^{2+}$).

X-ray Crystal Structure Determination. Crystals of both complexes $\mathbf{1b(PF_6)_2}$ and $\mathbf{1c(PF_6)_2}$ were obtained by slow diffusion of diethyl ether into an acetone solution containing complex $\mathbf{1a(PF_6)}$ at room temperature and in the presence of atmospheric oxygen. The measured crystals were prepared under inert conditions immersed in perfluoropolyether as protecting oil for manipulation.

Data Collection. Crystal structure determinations for $\mathbf{1b(PF_6)_2}$ and $\mathbf{1c(PF_6)_2}$ were carried out using a Bruker-Nonius diffractometer equipped with an APEX II 4K CCD area detector, a FR591 rotating anode with Mo Kα radiation, Montel mirrors as monochromator, a Kappa 4-axis goniometer, and an Oxford Cryosystems low-temperature device Cryostream 700 plus (T = −173 °C). Full-sphere data collection was used with ω and φ scans. Programs used: Data collection with APEX-2,[12] data reduction with Bruker Saint,[13] and absorption correction with SADABS.[14]

Structure Solution and Refinement. Crystal structure solution was achieved using direct methods as implemented in SHELXTL[15] and

dx.doi.org/10.1021/ic501483s | Inorg. Chem. 2014, 53, 10394−10402

Scheme 1. Synthetic Strategy for Preparation of the Complexes Described in This Work[a]

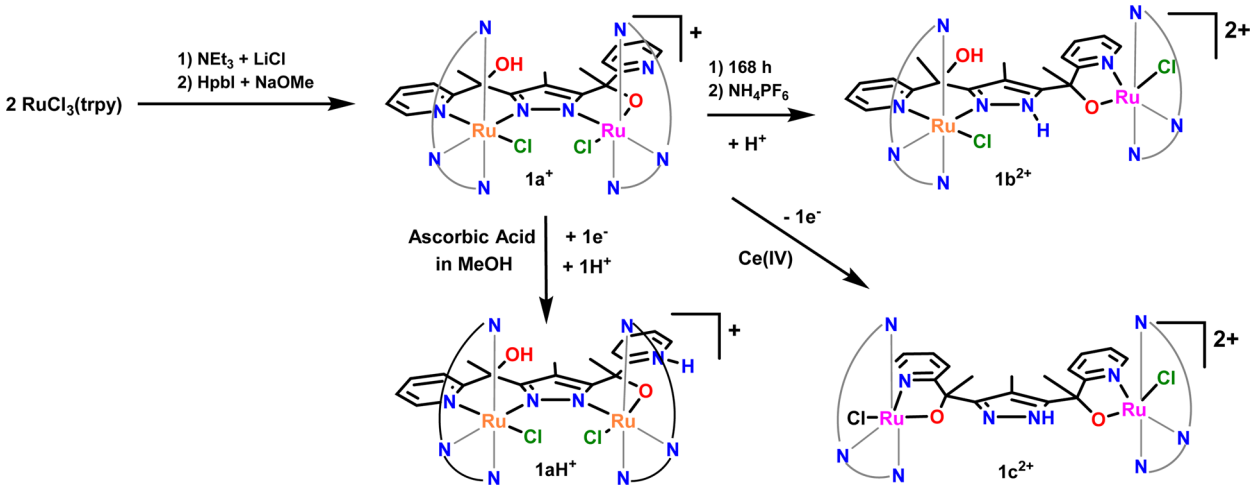

[a]The terpyridine ligand is represented with three N atoms linked by arcs. Color code for Ru: orange for oxidation state II, and fuchsia for oxidation state III. This color code is used from now on in all schemes.

Scheme 2. Structure of All Possible Isomeric Species for Dinuclear Ru^{II}–Cl Complexes Bearing the Hpbl and trpy Ligands

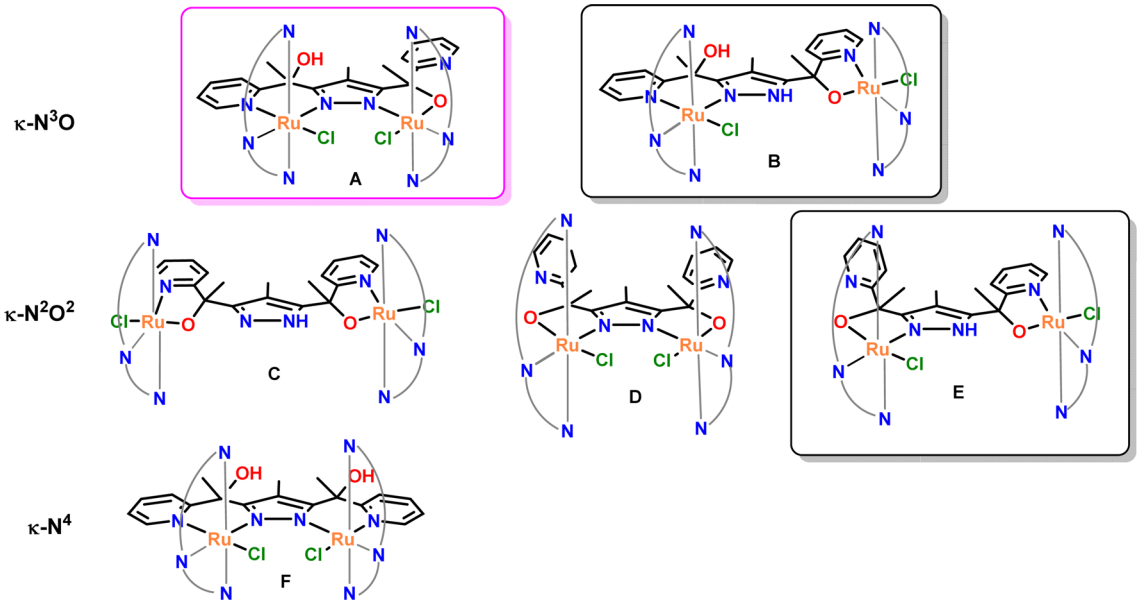

visualized using the program XP. Missing atoms were subsequently located from difference Fourier synthesis and added to the atom list. Least-squares refinement on F^2 using all measured intensities was carried out using the program SHELXTL. All non-hydrogen atoms were refined including anisotropic displacement parameters.

Comments to the Structures. Compound **1b**$(PF_6)_2$ crystallizes with 1 molecule of the metal complex, two PF_6^- anions, 2 acetone molecules, and 0.5 molecule of water in the asymmetric unit. One of the acetone molecules is disordered in two positions with a ratio of 53:47. The water molecule is also disordered (50:50) and shared with the neighboring unit cell. Compound **1c**$(PF_6)_2$ crystallizes with 1 molecule of the metal complex, 2 PF_6^- anions, and 2.5 molecules of water in the asymmetric unit. One of the PF_6^- anions is disordered in two positions (ratio 60:40). Water molecules are highly disordered with an occupancy of 1.00:0.75:0.50:0.125:0.125. As a consequence of this, the hydrogen atoms of the water molecules could not be precisely localized (B alert in the CheckCIF report).

RESULTS AND DISCUSSION

1. Synthesis and Structure. The dinuclear complex **1a**(PF_6) is prepared using $[RuCl_3(trpy)]$ as metal precursor in combination with the Hpbl ligand (Scheme 1) under inert conditions in a 2:1 $[RuCl_3(trpy)]$:Hpbl molar ratio with excess of MeONa as a base. Either reflux or microwave heating in MeOH can be used, giving similar results with moderate yields (27% for conventional reflux and 36% for microwave). Complex **1a**(PF_6) is then washed with hot CH_2Cl_2.

There are a number of potential Ru–Cl dinuclear complexes that can be obtained given the chelating, dinucleating hexadentate nature of the Hpbl ligand and assuming that the trpy ligands remain always bonded to the Ru metal center. Scheme 2 presents a drawing of all these potential isomers at oxidation state II, classified as a function of the N/O pbl^- chelating atoms, where pbl^- ligand can have different degrees of protonation.

dx.doi.org/10.1021/ic501483s | Inorg. Chem. 2014, 53, 10394–10402

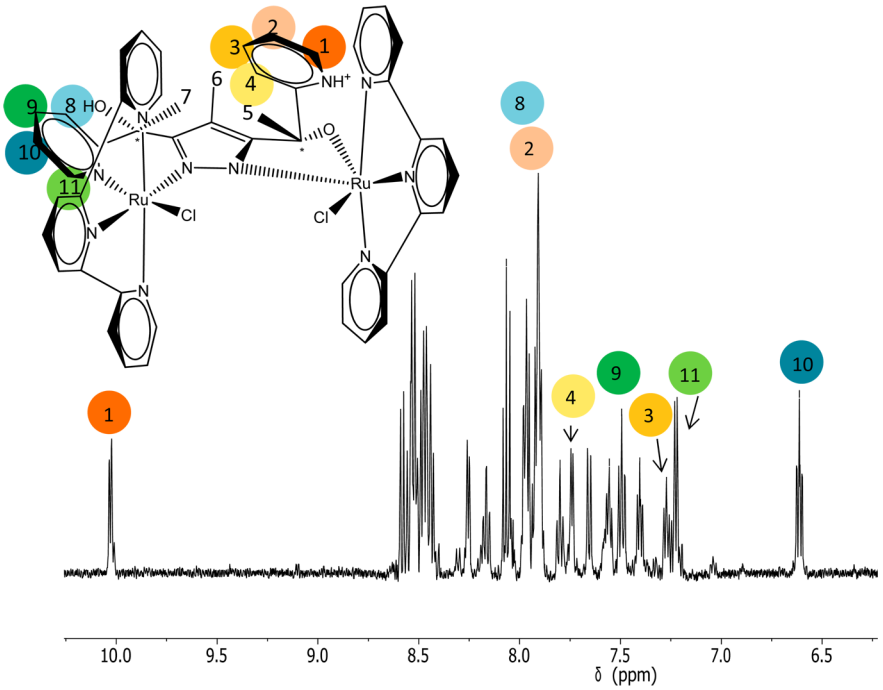

Figure 1. ^{1}H NMR spectra for complex **1aH**$^+$ in MeOD generated from addition of ascorbic acid to **1a**$^+$ and numbering scheme.

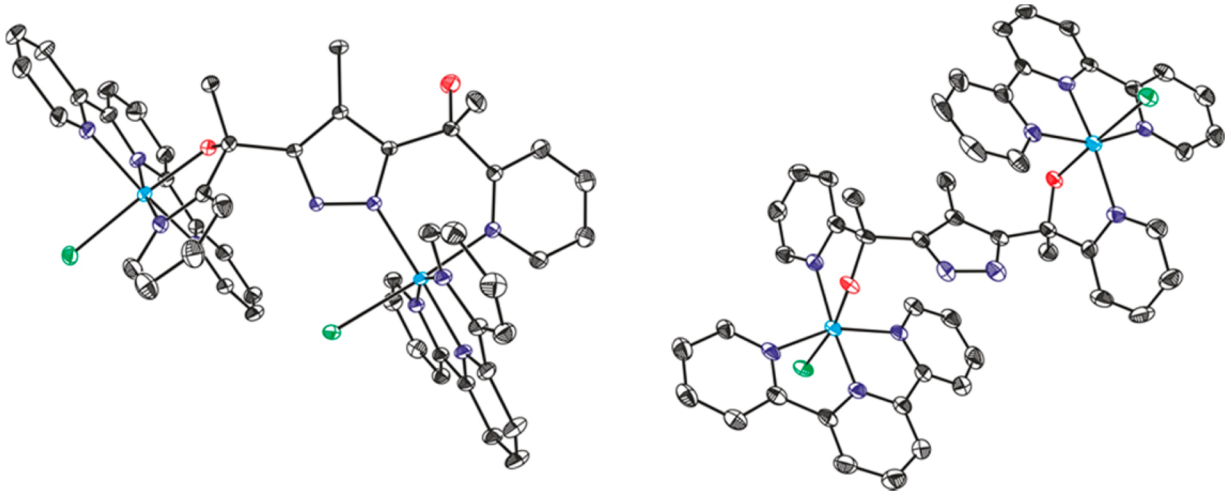

Figure 2. ORTEP plots (thermal ellipsoids at 50% probability) for X-ray crystal structures of the cationic part of the complexes: **1b**$^{2+}$ (left) and **1c**$^{2+}$ (right). Hydrogen atoms have been omitted for clarity. Color codes: C, black; Cl, green; N, dark blue; O, red; Ru, light blue.

From a geometrical perspective it is interesting to realize that species C, D, and F (Scheme 2) contain a C_2 rotation axis that bisects the pyrazolyl moiety of the pbl$^-$ ligand, whereas species A, B, and E have no symmetry elements except for the identity, "*E*". This is important since analytic techniques such as NMR allow us to discern between symmetric and nonsymmetric species. The ^{1}H NMR spectrum of the dinuclear complex **1a**$^+$ presents broad resonances (see Figure S1 in the Supporting Information), suggesting the paramagnetic nature of the Ru(II)−Ru(III) complex. This is further confirmed by the open-circuit potential situated above the first oxidation wave (see below). Addition of a reducing agent such as ascorbic acid to a NMR tube containing this paramagnetic complex generates the diamagnetic **1aH**$^+$ complex, whose ^{1}H NMR spectrum is presented in Figures 1 and S2 in the Supporting Information. On the basis of the number of resonances and their integration, the NMR is consistent with a nonsymmetric complex containing two terpyridines and one Hpbl ligand. Accordingly, the symmetric species (C, D, and F, Scheme 2) are discarded.

For Ru−Hbpp complexes we have a substantial number of both mononuclear and dinuclear complexes[7a,9a,b,10,16] that have been thoroughly characterized by ^{1}H NMR spectroscopy. For these complexes the trans influence of the Ru−Cl group induces the presence of a pseudotriplet at 6−7 ppm due to the pyridyl group of the Hbpp ligand. The fact that in the present case we only find one triplet in this region suggests that one pyridyl of pbl$^-$ is coordinated whereas the other one is not. The noncoordinated Hpbl pyridyl group at low pH is protonated, and this produces the appearance of a doublet above 10.0 ppm due to the CH alpha to the pyridyl N atom. The Ru−Cl trans to the pyridyl group of the pbl$^-$ ligand is confirmed by the absence of a second resonance in this region. If the Ru−Cl were

dx.doi.org/10.1021/ic501483s | *Inorg. Chem.* 2014, 53, 10394−10402

trans to the *N*-pyrazolyl moiety then the Ru−Cl group would interact with the H alpha to the coordinated *N*-pyridylic group of the pbl$^-$ ligand that would be strongly shifted downfield toward the 9.5−10 ppm region. In addition, given the substitutionally inert nature of Ru(II) in this type of complexes,[10] the ligand arrangement found in the X-ray structure of **1b**$^{2+}$ (see Figure 2) further confirms the trans disposition of the Ru−Cl group with regard to the *N*-pyridylic group of the bpl$^-$ ligand. All this is also in agreement with the experimental potentials found in the CV which indicate a N_5 type of coordination environment for one of the Ru metal centers and a ON_4(Pz) for the second one, as will be detailed later on. This discards species B and E as potential candidates. Finally and in addition to the previous arguments, electrochemistry allows discriminating between species A and E. A wave at 0.78 V associated with a Ru first coordination sphere environment of 5 *N*-pyridyl and Cl appears in the cyclic voltammetry, which allows us to assign this complex to species A since species E would have a much lower redox potential given the alkoxo coordination of its Ru centers (vide infra) (Table 1).[10] Furthermore, the complex has been characterized by UV−vis and MS techniques (See Figures S7, S8, and S10 in the Supporting Information).

Table 1. Electrochemical Data for Mononuclear[10] and Dinuclear Hpbl Complexes[a]

entry	complex[b]	$E_{1/2}$ vs SSCE in V Ru(III/II)
1[b]	[**Ru**−N_5−H_2O]$^{2+}$ [10]	0.72
2[b]	[**Ru**−ON_4(Pz)−H_2O]$^{2+}$ [10]	0.24
3[b]	[**Ru**−ON_4(Py)−H_2O]$^{2+}$ [10]	0.38
4[c]	[Cl−(Pz)N_4O−Ru-**Ru**−N_5−Cl]$^+$, **1a**$^+$	0.78
5[c]	[Cl−(Pz)N_4O−**Ru**-Ru−N_5−Cl]$^+$, **1a**$^+$	0.07
6[c]	[Cl−(Py)N_4O−Ru-**Ru**−N_5−Cl]$^{2+}$, **1b**$^{2+}$	0.78
7[c]	[Cl−(Py)N_4O−**Ru**-Ru−N_5−Cl]$^{2+}$, **1b**$^{2+}$	0.3
8[c]	[Cl−(Py)N_4O−**Ru-Ru**−ON_4(Py)−Cl]$^{2+}$, **1c**$^{2+}$	0.3

[a]Bold font indicates the metal center undergoing the redox process. Complexes are labeled indicating the atoms at the first Ru coordination sphere. The trpy ligands are thus represented by N_3 and the pbl$^-$ ligand either by N_2 or by one NO (N(Py) when coordinated by the pyridyl group or N(Pz) by the pyrazolyl). Finally, the H_2O or Cl ligands are explicitly written. [b]In 0.1 M of triflic acid aqueous solution. [c]In 0.1 M of TBAH in MeOH.

Complex **1a**$^+$ slowly isomerizes into **1b**$^{2+}$ in MeOH at room temperature (1 week), substituting the initial coordinated pyrazolyl moiety from pbl$^-$ by the free pyridyl on the alkoxo side and generating a Ru^{III}−ON_4(Py) moiety (Scheme 1). An X-ray structure of this new complex is presented in Figure 2 that will be discussed below. The UV−vis spectrum, the CV, and the MS spectrum are shown in Supporting Information Figures S4, S8, and S11, respectively.

Addition of 1 equiv of Ce(IV) to a methanolic solution of the mixed-valence Ru^{III}−Ru^{II} complex **1a**$^+$ at room temperature generates the dinuclear complex **1c**$^{2+}$ where both Ru centers are now at oxidation state III,III. The first coordination sphere of the latter is Ru^{III}−ON_4(Py), which is with alkoxo coordination, with the two pyridyls from the pbl$^-$ ligands also coordinated. In addition, the N atoms of the pyrazolate moiety are not involved in the metal coordination as can be seen in the crystal structure in Figure 2 and also in a drawing in Scheme 1 (see Figures S5, S9, and S12 in the Supporting Information for further characterization).

The solid state structure for the cationic parts of **1b**$^{2+}$ and **1c**$^{2+}$ are very similar to related low-spin d^6 Ru(II) and low-spin d^5 Ru(III) complexes previously published in the literature showing pseudo-octahedral geometry (Figure 2, Table 2).[6−9]

Table 2. Crystallographic Data for Complexes [1b$(PF_6)_2$]·$(C_3H_6O)_2$·$(H_2O)_{0.5}$ and [1c$(PF_6)_2$]·$(H_2O)_{2.5}$

compound	[**1b**]$(PF_6)_2$·$(C_3H_6O)_2$·$(H_2O)_{0.5}$	[**1c**]$(PF_6)_2$·$(H_2O)_{2.5}$
formula	$C_{54}H_{54}Cl_2F_{12}N_{10}O_{4.5}P_2Ru_2$	$C_{48}H_{44}Cl_2F_{12}N_{10}O_{4.5}P_2Ru_2$
solvent detected	1/2H_2O + 2acetone	2.5H_2O
fw	1478.05	1395.91
cryst size (mm^3)	0.50 × 0.20 × 0.05	0.20 × 0.10 × 0.05
cryst color	brown	red
temp (K)	100	100
cryst syst	triclinic	triclinic
space group	$P\bar{1}$	$P\bar{1}$
a (Å)	12.5295(6)	13.2322(9)
b (Å)	14.6459(7)	15.2695(10)
c (Å)	18.2104(9)	15.8750(10)
α (deg)	107.284(2)	70.027(2)
β (deg)	109.045(2)	68.822(2)
γ (deg)	96.360(2)	89.430(2)
V (Å^3)	2935.2(2)	2787.4(3)
Z	2	2
ρ (g/cm^3)	1.672	1.663
μ (mm^{-1})	0.754	0.789
θ_{max} (deg)	36.60	26.38
no. of reflns measd	101 293	24 599
no. of unique reflns obsd	20 024 [R_{int} = 0.0696]	8054 [R_{int} = 0.0853]
abs corr	SADABS	SADABS
trans. min/max	0.871/1.000	0.703/0.962
parameters	834	845
R1/wR2 [$I > 2\sigma(I)$]	0.0415/0.0980	0.0568/0.1537
R1/wR2 [all data]	0.0758/0.1186	0.0873/0.1796
goodness-of-fit (F^2)	1.037	1.036
peak/hole (e/Å^3)	1.235/−0.977	1.373/−1.002

For complex **1b**$^{2+}$ it is interesting to realize that the pyrazolyl-coordinating side generates a 6-membered ring metallacycle with the Ru metal center, whereas the other metal center with no pyrazolyl coordination generates a 5-membered ring. This can be an important factor in the isomerization driving force.[17] In addition, this new coordination environment produces a large separation between the two Cl ligands that are now situated at 6.8 Å. This is important from a reactivity perspective because it will preclude an intramolecular interaction between potential active sites derived from their substitution. The latter is even more strongly manifested in the crystal structure of **1c**$^{2+}$, where now the two Ru−Cl bonds are situated trans to one another with a Cl−Cl distance of 12.7 Å.

2. Redox Chemistry and Linkage Isomerism. The electrochemical behavior of the dinuclear complex **1a**$^+$ has also been studied by cyclic voltammetry in MeOH, and the potential complexes generated and their generation routes are mapped in Scheme 3.

dx.doi.org/10.1021/ic501483s | *Inorg. Chem.* 2014, 53, 10394−10402

Scheme 3. Schematic Representation of the Different Linkage Isomerization Processes Taking Place for $1a^+$ and Its $1e^-$ Oxidized and Reduced Species[a]

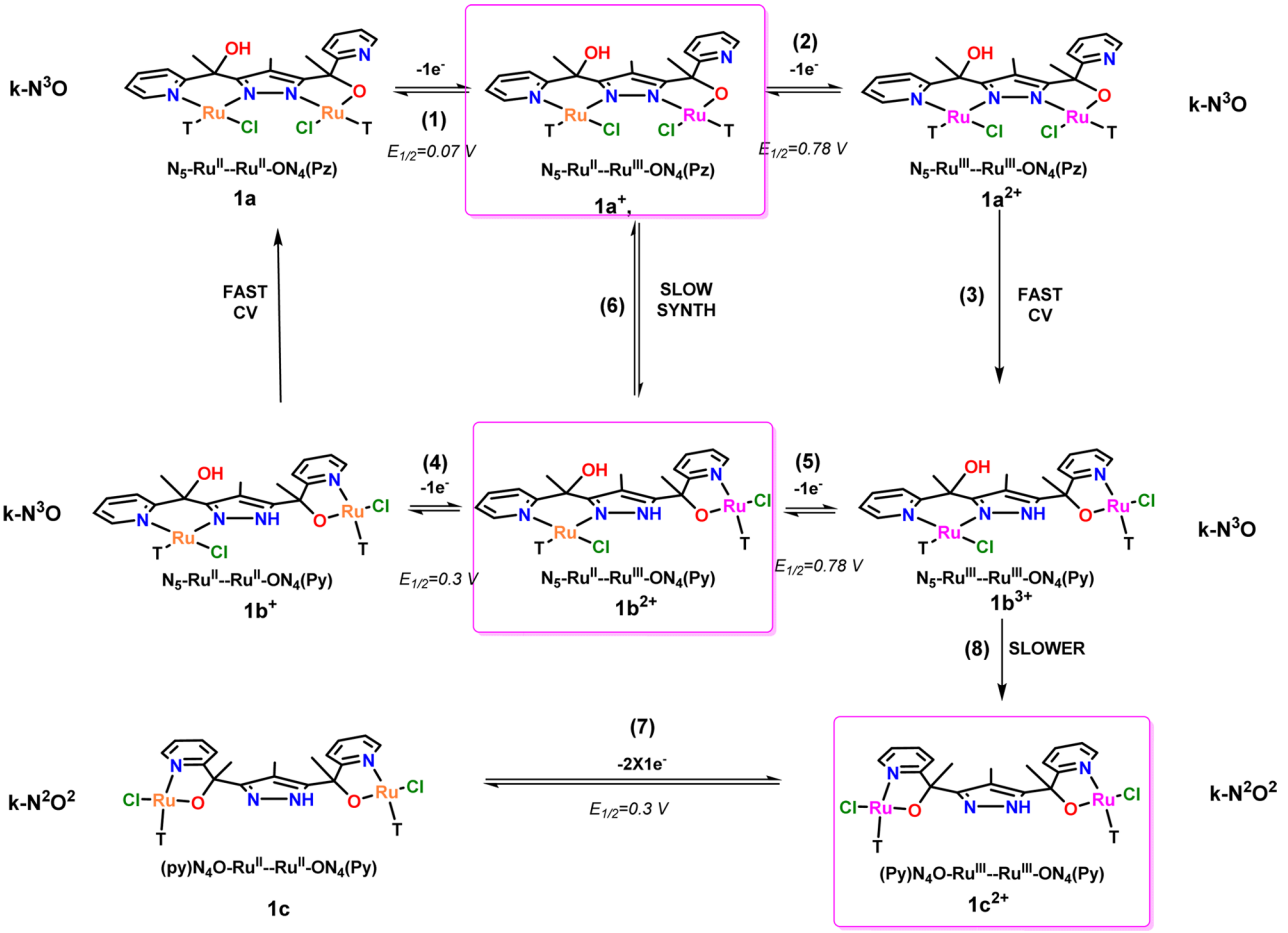

[a]Here the terpyridine ligand is represented by "T", and its axial coordination positions are not shown for clarity purposes.

In order to facilitate the tracking of the different species generated electrochemically we are using a nomenclature that only shows the first coordination sphere. In this nomenclature the Cl ligands are not shown since they are always coordinated as are the trpy ligands that are displayed with three N. The other two positions for the octahedral coordination of the Ru metal center are occupied by the pbl^- ligand. They can be either the alkoxo moiety labeled O or the pyridyl labeled as N(Py) or the pyrazolyl labeled as N(Pz). In the case where both pyridyl and pyrazolyl groups are coordinated, they are labeled with two N. For instance, $\mathbf{1a}^+$ is labeled as $N_5{-}Ru^{II}{-}Ru^{III}{-}ON_4(Pz)$, as indicated in Scheme 3.

Figure 3a shows the cyclic voltammograms obtained for $\mathbf{1a}^+$ scanning anodically at 400 mV/s. The first scan shows the presence of two quasireversible waves at $E_{1/2}$ = 0.07 ($E_{p,a}$ = 0.12 V, $E_{p,c}$ = −0.03 V, ΔE = 150 mV) and 0.78 V ($E_{p,a}$ = 0.84 V, $E_{p,c}$ = 0.73 V, ΔE = 110 mV), which are assigned to the following redox couples

$$\underset{\mathbf{1a}^+}{N_5\text{-}Ru^{II}\text{--}\mathbf{Ru^{III}}\text{-}ON_4(Pz)} + 1e^- \longrightarrow \underset{\mathbf{1a}}{N_5\text{-}Ru^{II}\text{--}\mathbf{Ru^{II}}\text{-}ON_4(Pz)} \quad E_{1/2} = 0.07\ V \quad (1)$$

$$\underset{\mathbf{1a}^{2+}}{N_5\text{-}\mathbf{Ru^{III}}\text{--}Ru^{III}\text{-}ON_4(Pz)} + 1e^- \longrightarrow \underset{\mathbf{1a}^+}{N_5\text{-}\mathbf{Ru^{II}}\text{--}Ru^{III}\text{-}ON_4(Pz)} \quad E_{1/2} = 0.78\ V \quad (2)$$

The equation numbering is in accordance with Scheme 3. In addition, the Ru metal undergoing a change in oxidation state is marked in bold. This assignment is based on related mononuclear complexes that contain exactly the same first coordination environment for the Ru center (Table 1). In addition, the one-electron nature of the process at $E_{1/2}$ = 0.07 V was corroborated by bulk electrolysis (see Supporting Information Figure S3).

As repetitive cycles are carried out the presence of a new wave at $E_{1/2}$ = 0.30 V ($E_{p,a}$ = 0.38 V, $E_{p,b}$ = 0.17 V, ΔE = 210 mV) appears, which is associated with the linkage isomerization that occurs when the *N*-pyrazolyl is replaced by the *N*-pyridyl group once the Ru(III,III) species are reached, that is

$$\underset{\mathbf{1a}^{2+}}{N_5\text{-}Ru^{III}\text{--}Ru^{III}\text{-}ON_4(Pz)} \overset{k_1}{\rightleftharpoons} \underset{\mathbf{1b}^{3+}}{N_5\text{-}Ru^{III}\text{--}Ru^{III}\text{-}ON_4(Py)} \quad (3)$$

This newly generated species has one wave at 0.30 V as indicated previously

dx.doi.org/10.1021/ic501483s | *Inorg. Chem.* 2014, 53, 10394−10402

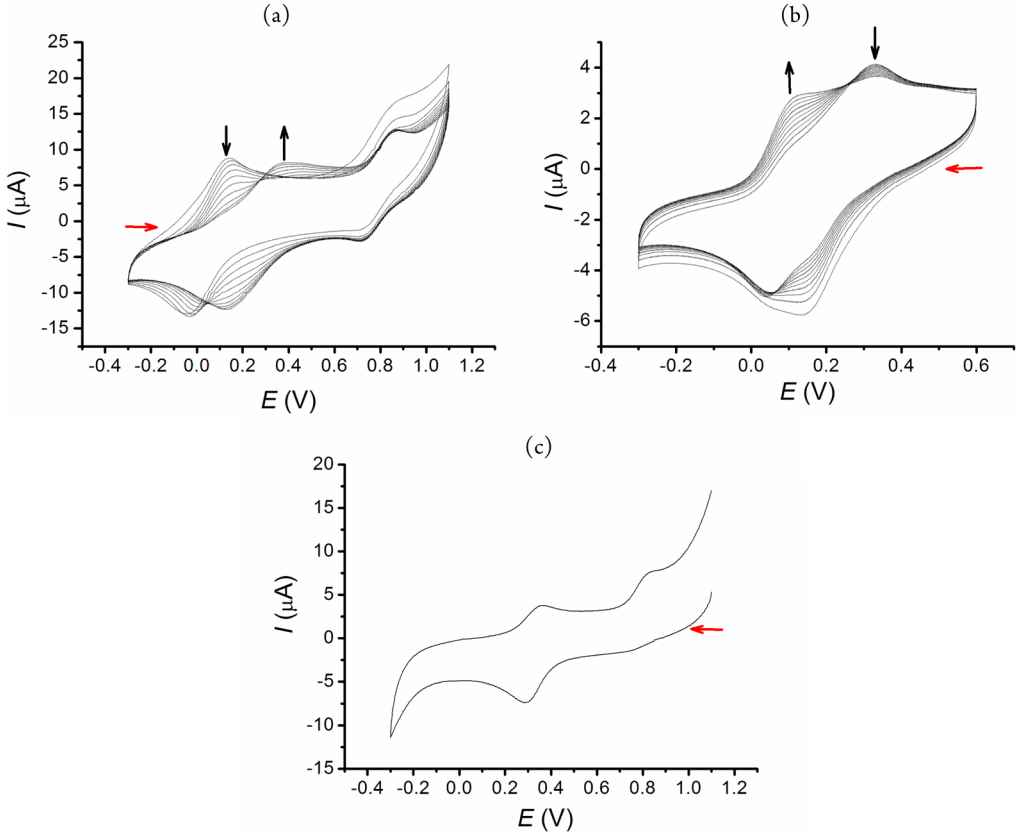

Figure 3. Cyclic voltammograms of complex $\mathbf{1a}^{+}$ in 0.1 M TBAH in MeOH at different scan rates and scanning directions (red arrows). Black arrows indicate the intensity increase or decrease: (a) scanning anodically at a scan rate of 400 mV/s with a previous equilibration time of 20 min at −0.30 V, (b) scanning cathodically at a scan rate of 200 mV/s and with an equilibration time of 45 min at 0.60 V, and (c) 50 mV/s scanning cathodically after holding the potential at 1.10 V for 3 min.

$$\underset{\mathbf{1b}^{2+}}{N_5\text{-}Ru^{II}\text{--}\mathbf{Ru}^{III}\text{-}ON_4(Py)} + 1e^- \longrightarrow \underset{\mathbf{1b}^{+}}{N_5\text{-}Ru^{II}\text{--}\mathbf{Ru}^{II}\text{-}ON_4(Py)} \quad E_{1/2} = 0.30\ V \quad (4)$$

and the second one that appears at the same potential as the parent complex

$$\underset{\mathbf{1b}^{3+}}{N_5\text{-}\mathbf{Ru}^{III}\text{--}Ru^{III}\text{-}ON_4(Py)} + 1e^- \longrightarrow \underset{\mathbf{1b}^{2+}}{N_5\text{-}\mathbf{Ru}^{II}\text{--}Ru^{III}\text{-}ON_4(Py)} \quad E_{1/2} = 0.78\ V \quad (5)$$

An authentic sample of $\mathbf{1b}^{2+}$ prepared independently gives exactly the same CV (see Figure S8 in the Supporting Information).

The 230 mV difference in redox potentials from the N-Py to N-Pz (entries 5 and 7 in Table 1) is a phenomenon that we observed earlier for related mononuclear complexes as displayed in Table 1 (compare entries 2 and 3) and is due to the stronger σ-donation and less π-accepting character of the pyrazolyl vs the pyridyl group.

After 10 scans complex $\mathbf{1a}^{2+}$ is totally transformed into $\mathbf{1b}^{3+}$, as can be observed in Figure 3a, where the wave at 0.07 V has totally disappeared. The reverse isomerization process occurs upon scanning in the 0.60 to −0.30 V region as shown in Figure 3b, that is by avoiding generation of oxidation state III for the RuN_5 moiety that as mentioned earlier is responsible for the opposite process

$$\underset{\mathbf{1b}^{2+}}{N_5\text{-}Ru^{II}\text{--}Ru^{II}\text{-}ON_4(Py)} \underset{}{\overset{k_2}{\rightleftharpoons}} \underset{\mathbf{1a}^{+}}{N_5\text{-}Ru^{II}\text{--}Ru^{II}\text{-}ON_4(Pz)} \quad (6)$$

Thus, at oxidation state III,III the isomerization from N-Pz to N-Py is favored, whereas at oxidation state II,II the opposite from N-Py to N-Pz is favored, which is a bit counterintuitive.

Another interesting feature of this system is observed when a CV of $\mathbf{1a}^{+}$ is performed after holding the potential at 1.10 V for 3 min as shown in Figure 3c. As it can be observed in the cathodic scan that the wave at 0.78 V has completely disappeared, and only one wave at 0.30 V is observed. This is consistent with generation of species $\mathbf{1c}^{2+}$, as corroborated with a CV prepared from an authentic sample. Thus, the wave observed now is due to

$$\underset{\mathbf{1c}^{2+}}{(Py)N_4O\text{-}\mathbf{Ru}^{III}\text{--}\mathbf{Ru}^{III}\text{-}ON_4(Py)} + 2\ e^- \longrightarrow \underset{\mathbf{1c}}{(Py)N_4O\text{-}\mathbf{Ru}^{II}\text{--}\mathbf{Ru}^{II}\text{-}ON_4(Py)} \quad E_{1/2} = 0.30\ V \quad (7)$$

Since the starting material is $\mathbf{1a}^{+}$ and we indicated earlier that after one-electron removal to form $\mathbf{1a}^{2+}$ this species quickly isomerizes to $\mathbf{1b}^{3+}$, it seems reasonable that $\mathbf{1b}^{3+}$ in turn also isomerizes to $\mathbf{1c}^{2+}$ but at a slower rate than the former

dx.doi.org/10.1021/ic501483s | Inorg. Chem. 2014, 53, 10394−10402

$$\underset{\mathbf{1b^{3+}}}{N_5\text{-}Ru^{III}\text{--}Ru^{III}\text{-}ON_4(Py)} \underset{}{\overset{k_3}{\rightleftharpoons}} \underset{\mathbf{1c^{2+}}}{(Py)N_4O\text{-}Ru^{III}\text{--}Ru^{III}\text{-}ON_4(Py)} \quad (8)$$

3. Catalytic Activity. Complex $\mathbf{1a}^+$ has been tested with regard to its ability to oxidize *cis*-β-methylstyrene together with related mononuclear complexes of formula $[Ru^{II}Cl(Hpbl)(trpy)]^+$,[10] and the results are reported in Table 3. The table also contains the performance of related complexes such as *in*-$[Ru^{II}(trpy)(Hbpp)(H_2O)]^+$,[16c] $\{[Ru^{II}(trpy)]_2(\mu\text{-}CH_3COO)(\mu\text{-}bpp)\}^{2+}$,[16b] $\{[Ru^{II}(trpy)(H_2O)]_2(\mu\text{-}pdz\text{-}dc)\}^{2+}$,[8a] and $\{[Ru^{II}(trpy)(H_2O)]_2(\mu\text{-}pyr\text{-}dc)\}^+$[8c] for comparison purposes.

Table 3. Catalytic Epoxidation of *cis*-β-Methylstyrene with PhIO by Means of $\mathbf{1a}^+$ and Related Mono- and Dinuclear Complexes for Purposes of Comparison[a]

catalyst	conv. (%)	[Epox], M cis/trans selectivity[b] (%)	TN[c]	TOF_i[d]	ref
$\mathbf{1a}^+$	100	0.71 (94)	401	39	this work
$\{[Ru(trpy)]_2(\mu\text{-}OOCH_3)(\mu\text{-}bpp)\}^{2+}$	100	0.80 (93)	452	36	this work
in-$[RuCl(Hpbl)(trpy)]^+$	100	0.74 (92)	499	22	this work
in-$[Ru(trpy)(Hbpp)(H_2O)]^+$	100	0.81 (56)	458	20	this work
$\{[Ru(trpy)(H_2O)]_2(\mu\text{-}pdz\text{-}dc)\}^{2+}$	92	1.32 (100)	1320	660	8a
$\{[Ru^{II}(trpy)(H_2O)]_2(\mu\text{-}pyr\text{-}dc)\}^+$	100	0.98 (100)	980	9180	8c

[a]Reaction conditions, cat. 1.0 mM for mononuclear and 0.5 mM for dinuclear complexes/alkene 1.0 M/$PhI(OAc)_2$ 2.0 M/H_2O 2.0 M/biphenyl 0.4 M/1,2-dichloroethane up to a final volume of 1.4 mL. [b]Cis/trans epoxide selectivity [c]TN is the turnover number with regard to epoxide formation. [d]TOF_i is the initial turnover frequency expressed in epoxide cycles per hour.

As general methodology, catalytic reactions have been carried out using a Cat:Subs:Ox ratio of 1:1000:2000 (mononuclear catalysts) or 1:2000:4000 (dinuclear catalysts) using PhIO as oxidant. The latter as well as formation of the corresponding Ru−OH_2 and its active higher oxidation state Ru=O species, from Ru−Cl, is favored by allowing it to stir at room temperature for 120 min before adding the corresponding substrate. The product distribution of the catalytic reaction was monitored by GC and GC-MS.

Milder and environmentally benign oxidants such as H_2O_2 or tBuOOH are usually able to oxidize Ru(II) to Ru(III) but not Ru(III) to Ru(IV) in this type of complexes. Since Ru(IV) is the active species for the epoxidation reaction,[8a,c] no substrate oxidation is observed using these peroxides.

In all cases the catalysts activity observed is very high, leading to substrate transformations of 100%. The product distribution observed is basically the epoxide and the products derived from C−C bond scission such as benzaldehyde.

Complex $\mathbf{1a}^+$ generates a 0.71 M concentration of *cis*-β-methylstyrene oxide after 16 h. Similarly, its mononuclear Ru−Hpbl counterpart, *in*-$[RuCl(Hpbl)(trpy)]^+$, produces a final epoxide concentration of 0.74 M after 20 h.

The catalytic activity observed here for the binuclear $\mathbf{1a}^+$ is comparable to that of several mononuclear complexes earlier described in the literature.[6a,b,8b] This is due to the fact that once the high oxidation states are accessed the linkage isomerization process can occur very fast, generating $\mathbf{1c}^{2+}$ type of species. This hampers both the electronic communication between the two Ru centers (due to pyrazolyl decoordination) and the potential through-space interaction of the active Ru−oxo groups (see the X-ray structure of $\mathbf{1c}^{2+}$) that would otherwise confer a cooperative effect of the two Ru centers in complex $\mathbf{1a}^+$.

A second run was carried out isolating the catalyst upon addition of diethyl ether and repeating the same protocol. The results obtained were basically the same based on stereoselectivity, but the TNs were about 10−15% lower. This decrease is due to partial loss of catalyst during the operations for the recovery process and to a certain extent to potentially deactivation pathways. These results together with 100% substrate conversion indicate that the catalyst stability is relatively high.

A very interesting feature of these complexes is their capacity to reach very high *cis*/*trans*-epoxide stereoselectivity, giving in all cases more than 90% of the corresponding *cis*-epoxide (see Table 3).

Finally, as can be deduced from Table 3, the velocity at which the epoxidation reaction occurs is directly related to the multianionic nature of the backbone dinucleating ligand. In this respect the complex containing the μ-pyr-dc^{3-} ligand has by far the largest TOF.

CONCLUSIONS

Three dinuclear Ru−Cl complexes containing the Hpbl and trpy ligands, $\{[RuCl(trpy)]_2(\mu\text{-}pbl\text{-}\kappa\text{-}N^3O)\}^+$ ($\mathbf{1a}^+$), $\{[RuCl(trpy)]_2(\mu\text{-}Hpbl\text{-}\kappa\text{-}N^3O)\}^{2+}$ ($\mathbf{1b}^{2+}$), and $\{[RuCl(trpy)]_2(\mu\text{-}Hpbl\text{-}\kappa\text{-}N^2O^2)\}^{2+}$ ($\mathbf{1c}^{2+}$), have been prepared, isolated, and characterized by analytic and spectroscopic techniques. The coordination versatility of the Hpbl ligand allows the presence of multiple isomers that can be obtained depending on the Ru oxidation state and confers the system an extremely rich chemistry with regard to the potential isomers that can be obtained. In particular, fast N(Pz) → N(Py) (Hpbl acting from κ-N^3O) linkage isomerization is observed for the Hpbl ligand for $\mathbf{1a}^{2+}$ upon reaching oxidation state III,III. In sharp contrast, the opposite reaction occurs when oxidation state II,II is obtained. Finally, $\mathbf{1a}^+$ and its recently reported mononuclear analogue *in*-$[RuCl(Hpbl)(trpy)]^+$ have been tested as catalysts for epoxidation of *cis*-β-methylstyrene.

ASSOCIATED CONTENT

Supporting Information

Further spectroscopic (1D and 2D NMR) and spectroelectrochemical measurements for the reported complexes. This material is available free of charge via the Internet at http://pubs.acs.org.

AUTHOR INFORMATION

Corresponding Authors

*E-mail: lluis.escriche@uab.cat.
*E-mail: allobet@iciq.es.
*E-mail: xavier.sala@uab.cat.

Notes

The authors declare no competing financial interest.

■ ACKNOWLEDGMENTS

Support from MINECO (CTQ-2013-49075-R, CTQ2011-26440, and CTQ2011-23156-C02-02) is gratefully acknowledged. L.F. and R.M.G.-G. are grateful for the award of FI-UAB and PIF doctoral grants from UAB, respectively.

■ REFERENCES

(1) Hauser, S. A.; Cokoja, M.; Kühn, F. E. *Catal. Sci. Technol.* **2013**, *3*, 552−561.
(2) Cavani, F.; Teles, J. H. *ChemSusChem* **2009**, *2*, 508.
(3) In *Catalysts for fine chemical synthesis: Regio- and stereo-controlled oxidations and reductions*; Roberts, S. M., Whittall, J., Eds.; John Wiley Sons, Ltd.: England, 2007; Vol. *5*.
(4) (a) Sala, X.; Escriche, L.; Llobet, A. In *Molecular Solar Fuels*, 1st ed.; Wydrzynski, T. J., Hillier, W., Eds.; Royal Society of Chemistry, 2012; Chapter 10, pp 273−288. (b) Berardi, S.; Drouet, S.; Francas, L.; Gimbert-Surinach, C.; Guttentag, M.; Richmond, C.; Stoll, T.; Llobet, A. *Chem. Soc. Rev.* **2014**, DOI: 10.1039/C3CS60405E.
(5) (a) Meyer, T. J.; Huynh, M. H. V. *Inorg. Chem.* **2003**, *42*, 8140−8160. (b) Dovletoglou, A.; Adeyemi, S. A.; Meyer, T. J. *Inorg. Chem.* **1996**, *35*, 4120−4127. (c) Suen, H. F.; Wilson, S. W.; Pomerantz, M.; Walsh, J. L. *Inorg. Chem.* **1989**, *28*, 786−791. (d) Roecker, L.; Kutner, W.; Gilbert, J. A.; Simmons, M.; Murray, R. W.; Meyer, T. J. *Inorg. Chem.* **1985**, *24*, 3784−3791. (e) Takeuchi, K. J.; Thompson, M. S.; Pipes, D. W.; Meyer, T. J. *Inorg. Chem.* **1984**, *23*, 1845−1851. (f) Binstead, R. A.; Moyer, B. A.; Samuels, G. J.; Meyer, T. J. *J. Am. Chem. Soc.* **1981**, *103*, 2897−2899. (g) Moyer, B. A.; Meyer, T. J. *Inorg. Chem.* **1981**, *20*, 436−444. (h) Moyer, B. A.; Meyer, T. J. *J. Am. Chem. Soc.* **1978**, *100*, 3601−3603.
(6) (a) Sala, X.; Santana, N.; Serrano, I.; Plantalech, E.; Romero, I.; Rodríguez, M.; Llobet, A.; Jansat, S.; Gómez, M.; Fontrodona, X.; Eur, J. *Inorg. Chem.* **2007**, 5207−5214. (b) Serrano, I.; Sala, X.; Plantalech, E.; Rodríguez, M.; Romero, I.; Jansat, S.; Gómez, M.; Parella, T.; Stoeckli-Evans, H.; Solans, X.; Font-Bardia, M.; Vidjayacoumar, B.; Llobet, A. *Inorg. Chem.* **2007**, *46*, 5381−5389. (c) Sala, X.; Poater, A.; Romero, I.; Rodríguez, M.; Llobet, A.; Solans, X.; Parella, T.; Santos, T. M. *Eur. J. Inorg. Chem.* **2004**, 612−618.
(7) (a) Planas, N.; Christian, G. J.; Mas-Marza, E.; Sala, X.; Fontrodona, X.; Maseras, F.; Llobet, A. *Chem.—Eur. J.* **2010**, *16*, 7965−7968. (b) Aguiló, J.; Naeimi, A.; Bofill, R.; Mueller-Bunz, H.; Llobet, A.; Escriche, L.; Sala, X.; Albrecht, M. *New J. Chem.* **2014**, *38*, 1980−1987.
(8) (a) Di Giovanni, C.; Vaquer, L.; Sala, X.; Benet-Buchholz, J.; Llobet, A. *Inorg. Chem.* **2013**, *52*, 4335−4345. (b) García-Antón, J.; Bofill, R.; Escriche, L.; Llobet, A.; Sala, X. *Eur. J. Inorg. Chem.* **2012**, 4775−4789 and references therein. (c) Di Giovanni, C.; Poater, A.; Benet-Buchholz, J.; Cavallo, L.; Solà, M.; Llobet, A. *Chem.—Eur. J.* **2014**, *20*, 3898−3902.
(9) (a) Francàs, L.; Sala, X.; Escudero-Adán, E.; Benet-Buchholz, J.; Escriche, L.; Llobet, A. *Inorg. Chem.* **2011**, *50*, 2771−2781. (b) Francàs, L.; Sala, X.; Benet-Buchholz, J.; Escriche, L.; Llobet, A. *ChemSusChem* **2009**, *2*, 321−329. (c) Lopez, I.; Ertem, M. Z.; Maji, S.; Benet-Buchholz, J.; Keidel, A.; Kuhlmann, U.; Hildebrandt, P.; Cramer, C. J.; Batista, V. S.; Llobet, A. *Angew. Chem., Int. Ed.* **2014**, *53*, 205−209.
(10) Francàs, L.; González-Gil, R. M.; Poater, A.; Fontrodona, X.; García-Antón, J.; Sala, X.; Escriche, L.; Llobet, A. *Inorg. Chem.* **2014**, *53*, 8025−8035.
(11) Sullivan, B. P.; Calvert, J. M.; Meyer, T. J. *Inorg. Chem.* **1980**, *19*, 1404.
(12) *Data collection with APEX II*, version v2013.4-1; Bruker AXS Inc.: Madison, WI, 2007.
(13) *SAINT*, version V8.30c; Bruker AXS Inc.: Madison, WI, 2007.
(14) Blessing. *Acta Crystallogr.* **1995**, *A51*, 33−38. *SADABS*, V2012/1; Bruker AXS Inc.: Madison, WI, 2001.
(15) Sheldrick, G. M. *Acta Crystallogr.* **2008**, *A64*, 112−122. *SHELXTL*, versions V6.12 and 6.14.
(16) (a) Roeser, S.; Ertem, M. Z.; Cady, C.; Lomoth, R.; Benet-Buchholz, J.; Hammarström, L.; Sarkar, B.; Kaim, W.; Cramer, C. J.; Llobet, A. *Inorg. Chem.* **2011**, *51*, 320−327. (b) Sens, C.; Romero, I.; Rodríguez, M.; Llobet, A.; Parella, T.; Benet-Buchholz, J. *J. Am. Chem. Soc.* **2004**, *126*, 7798−7799. (c) Sens, C.; Rodríguez, M.; Romero, I.; Llobet, A.; Parella, T.; Benet-Buchholz, J. *Inorg. Chem.* **2003**, *42*, 8385−8394.
(17) (a) Porterfield, W. W. *Inorganic Chemistry: A Unified Approach*, 2nd ed.; Academic Press, Inc.: San Diego, 1993. (b) Mackay, K. M.; Mackay, R. A. *Introduction to Modern Inorganic Chemistry*, 4th ed.; Blackie Academic & Professional: Glasgow, U.K., 1989.